RMetS

Royal Meteorological Society

Assessment of 1 month forecasts of weak Indian monsoons based on the NCEP Climate Forecast System (CFS)

Basanta Kumar Samala,[a]* R. Krishnan[b] and Mathew Roxy[b]

[a] *CES, Centre for Development of Advanced Computing, Pune, India*
[b] *Centre for Climate Change Research, Indian Institute of Tropical Meteorology, Pune, India*

ABSTRACT: This study focuses on analyses and validation of 1 month forecasts (OMFs) of weak Indian monsoons based on 10 member ensemble hindcasts (retrospective forecasts) of the NCEP Climate Forecast System (CFS) model for the period 1981–2008. The weak monsoon episodes chosen for the analysis correspond to summer monsoon months which were characterized by significant deficits in the All-India monthly rainfall of −20% of the climatological normal. Examination of the CFS-OMFs shows poor skill of the model in capturing the observed rainfall and circulation anomalies during weak monsoons. The present analysis suggests that deficiencies in realistically capturing the ocean-atmosphere coupling in the tropical Indian Ocean (IO) introduces biases in simulating sea surface temperature and rainfall anomalies in the equatorial region, which in turn affects the monsoon precipitation forecasts over the sub-continent. In particular, the mean thermocline in the near-equatorial IO is found to be practically flat in the CFS model, so that the near-equatorial anomalies in the model are not strong enough to weaken the summer monsoon circulation and reduce the monsoon precipitation over India. By examining a 100 year free run of the CFS model, it is seen that moderate monsoon-droughts simulated by the model have weak teleconnections with the equatorial IO dynamics. On the other hand, intense monsoon-droughts in the CFS-model are found be remarkably linked with the equatorial IO anomalies. It is suggested that improving the slope of the equatorial IO thermocline and allowing for more realistic IO-monsoon coupling in the CFS-model would be an important step for improving the skill of extended-range monsoon forecasts. Copyright © 2012 Royal Meteorological Society

KEY WORDS   Indian monsoon; weak monsoons; prolonged breaks; Indian Ocean coupling; Coupled model (CFS) forecasts

Received 9 November 2011; Revised 30 March 2012; Accepted 19 April 2012

1. Introduction

The South Asian monsoon sustains the lives of over one-fifth of the world's human population, which is heavily dependent on the seasonal summer monsoon rains during June to September. On average the seasonal monsoon rains over India contribute to nearly 75–80% of the annual precipitation. The year-to-year variations in the monsoonal rains exert significant impacts on agriculture, water resources, power generation, industry, transportation and various sectors of society, so that monsoon predictions at least one season in advance have enormous socio-economic implications (Sikka, 1999). In addition to the prediction of the seasonal mean monsoon, extended range forecasting of active and break monsoon spells on sub-seasonal (intra-seasonal) time-scales is an important issue. Low-frequency intra-seasonal variations of the Indian summer monsoon are characterized by organized northward propagating cloud-bands from the equator towards the continental landmass (Yasunari, 1979; Sikka and Gadgil, 1980) accompanied by large-scale anomalies of monsoon precipitation arising from feedbacks between the monsoon winds and moist convection (e.g. Krishnamurti and Subrahmanyam, 1982; Singh and Kripalani, 1985; Kripalani *et al.*, 1991; Wang and Xie, 1997; Krishnan *et al.*, 2000; Goswami and Ajaya Mohan, 2001; Goswami, 2005; Kulkarni *et al.*, 2011). Several investigators have attempted the problem of extended range monsoon predictability of active/break monsoon spells using statistical

models (e.g. Cadet and Daniel, 1988; Chen *et al.*, 1992; Webster and Hoyos, 2004; Xavier and Goswami 2007; Chattopadhyay *et al.*, 2008); as well as dynamical models (e.g. Krishnamurti *et al.*, 1990, 1992; Krishnan and Sundaram, 2007; Vitart and Molteni, 2009). Although improvements have taken place in short and medium-range forecasting during the last couple of decades, the progress in extended range dynamical forecasting of the monsoon intra-seasonal variations has been difficult to ascertain (Vitart and Molteni, 2009).

The prediction of active and break monsoons involves not only the sensitive dependence to initial conditions but also the manner in which the monsoonal evolution is influenced by slow processes such as ocean–atmosphere coupled interactions. Krishnamurti *et al.* (1990, 1992) demonstrated the feasibility of dynamical prediction of the monsoon low-frequency intra-seasonal variations by eliminating contaminations of the atmospheric initial state. Based on atmospheric general circulation model (AGCM) experiments, Waliser *et al.* (2003) estimated a limit of ∼25 days as the potential predictability for large-scale circulation parameters (e.g. 200 hPa velocity potential) of the summer monsoon intra-seasonal oscillation. Krishnan and Sundaram (2007) pointed out that the dynamical forecasts initiated from weak monsoon flow conditions exhibited higher potential predictability and slower growth of errors as compared to forecasts initiated from strong monsoon flow conditions. They suggested that prolonged monsoon breaks are potentially more predictable with longer lead times (2–3 weeks) as compared to active monsoon spells.

There is growing recognition about the importance of atmosphere-ocean coupled processes on the summer monsoon intraseasonal variations and their predictability. Observations

---

* Correspondence to: B. K. Samala, CES, C-DAC Main Building, Pune University Campus, Ganeshkhind, Pune-411007, India.
E-mail: basanta106@gmail.com

in the tropical Indian Ocean have clearly shown the importance of air–sea interactions in modulating the variations of sea surface temperature (SST) and turbulent fluxes on intra-seasonal time-scales (see Krishnamurti *et al.*, 1988; Sengupta and Ravichandran, 2001; Vecchi and Harrison, 2002; Roxy and Tanimoto, 2007, 2011). Krishnan *et al.* (2006) highlighted the significance of coupled interactions between the summer monsoon flow and the Indian Ocean circulation in driving prolonged monsoon breaks on intra-seasonal time-scales. The coupling basically involves a feedback in which an anomaly of the summer monsoon circulation induces downwelling and maintains a higher-than-normal heat-content in the Equatorial Eastern Indian Ocean (EEIO), so that the near-equatorial anomalies induce strong and sustained suppression of monsoon rainfall over the subcontinent through a weakening of the monsoon Hadley circulation. Modelling studies have emphasized the role of ocean-atmosphere coupling for improving the simulation of the boreal summer monsoon intra-seasonal variability (e.g. Fu *et al.*, 2007; Vitart and Molteni, 2009). Also, coupled models are being employed to produce monthly scale forecasts of atmospheric and oceanic parameters (e.g. Ferranti *et al.*, 1990; Vitart, 2004).

Coupled models are useful tools for enhancing the skill of seasonal forecasts and providing realistic simulations of tropical phenomena such as ENSO, IOD and the Indian summer monsoon (e.g. Krishna Kumar *et al.*, 2005; Wang *et al.*, 2005; Kang and Shukla, 2005; Behera *et al.*, 2006; Luo *et al.*, 2007, 2008a, 2008b; Krishnan *et al.*, 2010; Pattanaik and Kumar, 2010). In order to improve the skill of seasonal monsoon forecasts, it is important to not only capture the slow evolution of coupled phenomena such as ENSO and IOD, but also to provide a realistic depiction of coupled processes on intra-seasonal time-scales that can force extended active and break monsoon spells. For example, Joseph *et al.* (2010) noted that the coupled model forecasts by the Development of an European Multimodel Ensemble System for Seasonal to Interannual Prediction system (DEMETER - Palmer *et al.*, 2004) had limitations in capturing the observed relationship between monsoon droughts and very long breaks, and the associated air–sea interactions on intra-seasonal time scales. This eventually translated into poor forecasts of the seasonal monsoon rainfall over India. Drbholav and Krishnamurthy (2010) analysed the monthly mean retrospective forecasts of the boreal summer South Asian monsoon by the National Centers for Environmental Prediction (NCEP) climate forecast system (CFS – Version 1) model. They noted large errors in precipitation forecasts over the monsoon region during the June-July-August-September (JJAS) season even at 1 month lead times and these errors were found to grow somewhat as the lead increased. Pattanaik and Kumar (2010) have provided a comprehensive assessment of the skill of seasonal monsoon forecasts by the CFS model. The objective of the present work is to understand the fidelity of 1 month forecasts of the CFS in capturing the monsoon and Indian Ocean coupled interactions that often accompany prolonged breaks and weak monsoon conditions over the subcontinent (see Krishnan *et al.*, 2006).

2. Datasets and methodology

2.1. CFS model forecasts

This paper examines the skill of 1 month forecasts (OMFs) of all weak Indian summer monsoons during the period 1981–2008 by the NCEP CFS coupled model. The weak

monsoon episodes considered here are basically summer monsoon months which witnessed a significant deficit in the All-India monthly rainfall by at least −20% of the climatological normal. The atmospheric component of CFS is the NCEP atmospheric Global Forecast System (GFS) model (Moorthy *et al.*, 2001). The GFS is a global spectral model with triangular truncation of 62 waves (T62) in the horizontal (equivalent to nearly a 200 km Gaussian grid) and a finite differencing in the vertical with 64 sigma layers. The oceanic component of CFS is the GFDL Modular Ocean Model Version 3 (MOM3) (Pacanowski and Griffies, 1998), which is a finite difference version of the ocean primitive equations under the assumptions of Boussinesq and hydrostatic approximations. The ocean surface boundary is computed as an explicit free surface. The horizontal domain for the MOM3 is quasi-global, extending from 74°S to 64°N. The zonal resolution is 1° and the meridional resolution is 1/3° between 10°S and 10°N, gradually increasing through the tropics until becoming fixed at 1° poleward of 30°S and 30°N. There are 40 layers in the vertical with 27 layers in the upper 400 m, and the bottom depth is around 4.5 km. More details about the CFS model can be found in Saha *et al.* (2006).

An extensive set of retrospective forecasts (also referred to as hindcasts) of the CFS model, available for a 28 year period (1981–2008), is employed in the present analysis. Each forecast run of CFS is a full 9 month integration starting from 15 initial conditions that span for a month. Each month is divided into three segments centred on the pentad ocean initial conditions of the 11th and 21st of that particular month, and the first day of the following month. The 15 member ensemble atmospheric initial conditions are based on three sets of five continuous days in that month followed by a gap of 1 week after each 5 day block. The atmospheric initial conditions are from the NCEP Reanalysis-II (Kanamitsu *et al.*, 2002) and the ocean initial conditions are from the NCEP Global Ocean Data Assimilation System (GODAS) reanalysis. The OMFs in the present analysis are based on the CFS runs initiated from the first 10 initial conditions corresponding to the months May, June, July and August. For example, the CFS forecasts for June of a given year are initiated from the first 10 initial conditions in May of that particular year. The ensemble mean of first 10 members of CFS forecast starting from the previous month is considered as the mean OMF.

2.2. Validation datasets

The CFS model forecasts are validated against observed rainfall from CPC Merged Analysis of Precipitation (CMAP) global precipitation dataset which is constructed from rain gauge observations, satellite estimates and numerical model outputs (Xie and Arkin, 1996). Additionally, the study employs the observed monthly rainfall dataset over India based on Parthasarathy *et al.* (1994) available from the Indian Institute of Tropical Meteorology (IITM) dataset (Parthasarathy *et al.*, 1994, available at www.tropmet.res.in). The NCEP atmospheric Reanalysis II data (Kanamitsu *et al.*, 2002) and the NCEP Global Ocean Data Assimilation (GODAS) are also examined for validating the CFS forecasts. Table 1 provides information about weak monsoon months during 1981–2008 when the all India rainfall anomaly was >−20% of the climatological normal. In the following section, the diagnostic analysis of the CFS OMF and validation against observed/reanalysis datasets will be presented. The discussions here will address model biases in representing ocean-atmosphere coupled processes during weak monsoons and the prospects for improving the CFS forecasts.

Table 1. Cases of weak monsoon months during (1981–2008) when the deficit in the all India rainfall (AIR) exceeded by more than 20% of the climatological mean.

Weak monsoon month and year	All India Rainfall (AIR) anomaly	CMAP rainfall anomaly	CFS forecast (OMF) Rainfall anomaly
June 1982	−20.9	−37.7	−02.1
July 1982	−20.6	−07.1	−03.1
September 1982	−29.0	−13.9	−19.0
September 1986	−33.4	−07.3	−18.5
June 1987	−29.3	−12.2	−05.7
July 1987	−24.0	−37.4	−10.8
September 1987	−19.3	−25.6	−17.4
September 1991	−26.1	−28.1	−20.5
June 1992	−29.0	−10.0	−42.8
September 2000	−22.3	−28.2	28.4
August 2001	−22.0	−12.1	−05.9
September 2001	−34.4	−19.1	−14.5
July 2002	−56.8	−45.3	−00.6
September 2002	−22.1	−31.3	−08.5
July 2004	−19.4	−06.1	−10.1
September 2004	−24.4	−04.8	−00.7

The second, third and fourth columns are rainfall anomalies for AIR, CMAP and CFS forecast (OMF) respectively expressed as percentage departures from respective climatological mean. The CMAP and CFS anomalies are based on area-averages over the region (8–32 °N; 70–90 °E). The AIR anomalies are based on the IITM rainfall data (http://www.tropmet.res.in) for the period (1871–2008).

Section 4 provides an overall summary of the results of this study.

3. Diagnostic analyses of 1 month monsoon forecasts

3.1. Climatological features

Figure 1 shows a comparison of the JJAS mean climatology of rainfall and 10 m winds based on the OMF of the CFS model with the corresponding mean fields from the CMAP and NCEP reanalysis products. The summer monsoon rainfall maxima over the west coast of India, northern Bay of Bengal, northeast India and Myanmar region can be seen in the CFS OMF. It may be noticed that the model overestimates the precipitation over these regions as compared to the CMAP dataset, while the monsoon precipitation over central Bay of Bengal is underestimated in the model. The scanty precipitation over the rain-shadow region of southeast India and Tamilnadu is better captured in the CFS model. The model fails to capture the northwestward extent of central India rainfall zone adequately, whereas the CMAP rainfall is about 2–6 mm day^{-1} for the same region. The precipitation maximum in the EEIO region is also seen in the OMF. These systematic errors in the CFS forecasts, which manifest as deficient rainfall over India, excess rainfall over the Arabian Sea and the dipole-like pattern over the equatorial Indian Ocean, were also diagnosed by Drbholav and Krishnamurthy (2010). They further pointed out that the predictability errors of the CFS model over the EEIO grew as the forecast lead increased. It is encouraging to see that the monsoon surface winds pattern in the model is comparable with that of the NCEP reanalysis-II (Figure 1). The monsoon cross-equatorial flow and the Somali Jet are reasonably well captured, although the simulated southwesterly flow over the Bay of Bengal is slightly weaker compared to the NCEP reanalysis. Figure 2 shows a comparison of the JJAS mean SST between the model and GODAS. The features of SST spatial distribution are broadly similar with GODAS, although there is a warm model bias, particularly in the Arabian Sea and Bay of Bengal.

The basic question addressed here pertains to the ability of the CFS OMF in realistically capturing the ocean-atmosphere coupled feedbacks during anomalous weak monsoon episodes. The CFS OMF fields are available for the period 1981–2008. Using the observed Indian rainfall data from Parthasarathy et al. (1994), 16 cases of weak monsoon months were identified during 1981–2008 when the all India rainfall (AIR) deficit was below −20% of the climatological mean (see Table 1). The 20% threshold for selecting monthly rainfall anomalies is based on the consideration that the standard deviation of the monthly AIR for June, July, August and September corresponds to ∼22, ∼14, ∼16 and ∼22% of their respective monthly climatological means. Based on these monthly standard deviations, a 20% threshold has been used for selecting weak monsoon months. Monthly rainfall anomalies from the CMAP and CFS OMF datasets are computed from area-averages over the Indian monsoon region (8–32 °N, 70–90 °E) which includes both land and ocean points. Moreover, it must be noted that the AIR data are based on rainfall only over the land points of India
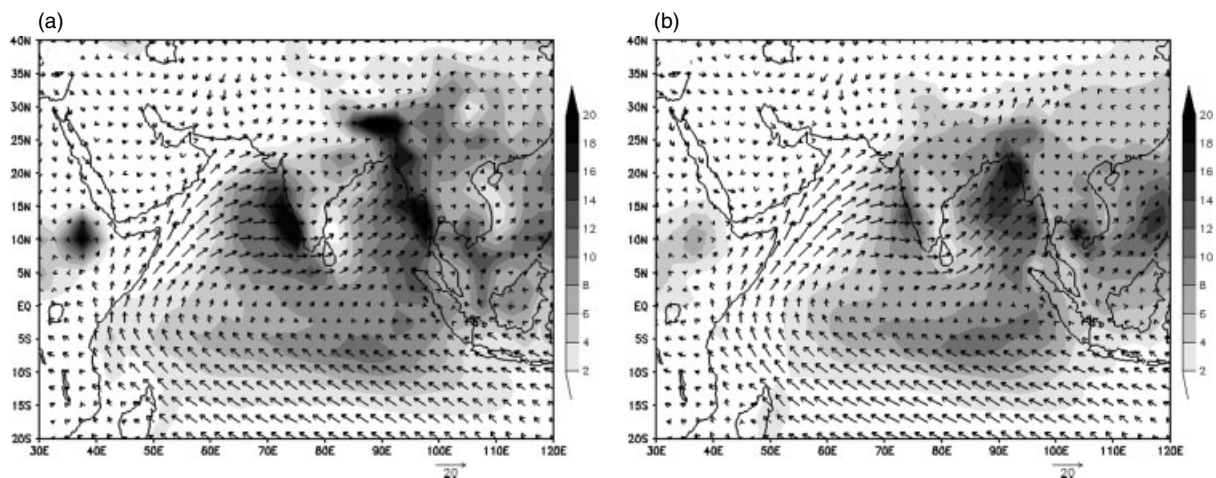

Figure 1. June, July, August, September climatological mean rainfall (mm day^{-1}) (shaded) and 10 m winds (ms^{-1}) (vector); (a) CFS 1 month forecast; (b) CMAP rainfall and NCEP reanalysis winds.
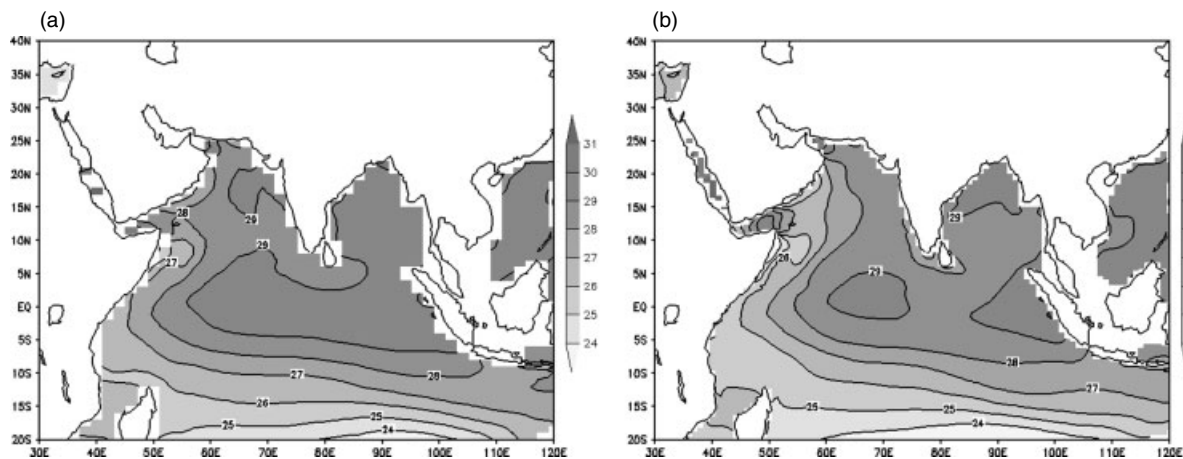
(a)

(b)

Figure 2. June, July, August, September climatological mean SST in °C; (a) CFS 1 month forecast; (b) GODAS.
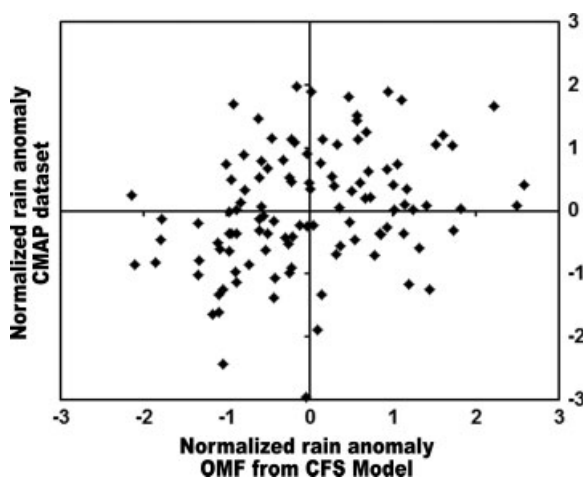
3.2.   Analysis of OMF of weak monsoons

Among the 16 weak monsoons in Table 1, it can be noticed that July 2002 had the largest deficiency of the all India rainfall (AIR) of about −57% departure from normal. It is intriguing to note that the OMF is unable to capture the magnitude of the large-scale rainfall deficiency during such an extreme monsoon drought. Examination of the spatial pattern of rainfall anomalies during July 2002 (Figure 4(a) and (b)) shows that the OMF of the rainfall anomaly over the Indian land region is almost out of phase with the CMAP anomalies. Although the rainfall deficiency over the eastern Arabian Sea can be noted in the OMF, the anomalies over central-north India, northeast India and the Bay of Bengal are almost opposite to the CMAP anomalies. The anomalous rainfall enhancement over EEIO during July 2002 and the equatorial westerly wind anomalies are qualitatively seen in the OMF.

A major forcing during the prolonged monsoon break in July 2002 was induced by the strong coupling of the anomalous monsoon circulation and IO dynamics as pointed out by Krishnan *et al.* (2006). Anomalous warming of the EEIO and enhancement of convection over the equatorial IO favours large-scale subsidence over the subcontinent leading to suppression of the monsoon Hadley cell and rainfall reduction over the Indian region (see Krishnan *et al.*, 2003, 2006). While the monsoon-Indian Ocean coupled interaction is one of the pathways for producing extended monsoon breaks, there are other plausible mechanisms that can sustain weak monsoon conditions. For example, extended monsoon breaks and droughts can be influenced by strong activity of the near-equatorial convectively-coupled phenomena such as the Madden Julian Oscillation (MJO) and ENSO (e.g. Sikka, 1999; Saith and Slingo, 2006; Joseph *et al.*, 2009; Neena *et al.*, 2011) and also by interactions with the mid-latitude circulation through intrusions of cold and dry air into the monsoon region (e.g. Ramaswamy, 1962; Bhat *et al.*, 2006; Krishnan *et al.*, 2009; Krishnamurti *et al.*, 2010). The skill of the CFS model in forecasting weak monsoons arising from equatorial IO coupled dynamics, can be understood by separating this category of weak monsoons from the rest of the weak monsoon cases. Six cases of weak monsoons that were accompanied by anomalous conditions in the equatorial IO were segregated based on examination of rainfall and SST anomalies individually for each of the 16 weak monsoons. These six weak monsoons correspond to September 1986, July 1987, September 1987, September 2000, September 2001 and July 2002.
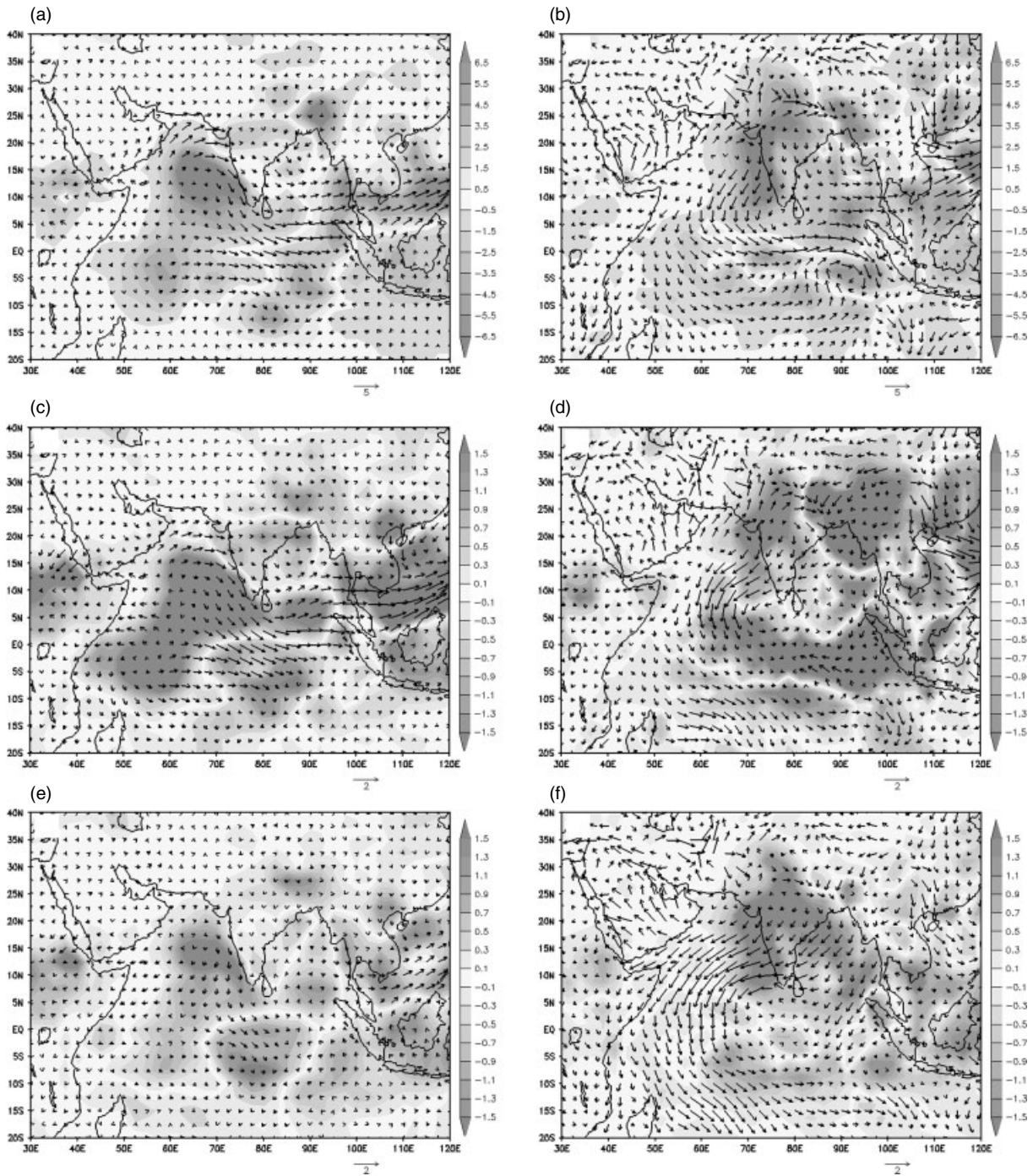

Figure 3. Scatter plot of normalized rainfall anomaly over Indian monsoon region (8–32 °N, 70–90 °E) from OMF of CFS model *versus* the CMAP observed dataset. The monthly rainfall anomalies for June, July, August and September from the CFS model and CMAP are normalized with respect to their respective monthly standard deviations.

The monthly rainfall datasets are for the period (1981–2008).

(Parthasarathy *et al.*, 1994). The monthly rainfall departures from the CMAP and CFS OMF for the 16 weak monsoon cases are given in Table 1. Although the negative sign of the rainfall anomaly is captured by the OMF for most of the weak monsoon cases, there are significant differences in the magnitudes of the anomalies between the OMF and observations (e.g. September 1991, June 1992, July 1992, August 2001, July 2002, September 2002). Figure 3 shows a scatter plot of OMF *versus* CMAP normalized rainfall anomalies over the Indian monsoon region for all 112 cases (i.e. 28 years × 4 months: corresponding to the June to September monsoon months over the period 1981–2008). It is noted that the correlation between the OMF and CMAP normalized anomalies is rather low ($r = 0.29$) indicating that the skill of the OMF is rather poor. In particular, one can see a significant scatter in the weak monsoon rainfall anomalies (i.e. third quadrant) between CMAP and OMF. It is further noted that the correlation coefficients between the OMF and CMAP anomalies for June, July, August and September are 0.30, 0.23, 0.37, 0.26 respectively, indicating that the skill of the OMF is comparable for the individual monsoon months.

Figure 4. Rainfall anomaly (mm day^{-1}) (shaded) and 10 m wind anomaly (m s^{-1}) (vector); (a,c,e) from CFS OMF and (b,d,f) from CMAP rainfall anomaly and NCEP reanalysis winds; (a,b) for July 2002; (c,d) mean of six cases (September 1986, July 1987, September 1987, September 2000, September 2001, July 2002); (e,f) composite mean of all weak monsoon months (from Table 1).

Composite maps of rainfall and low-level wind anomalies based on the above six weak monsoon cases from the OMF and observations are shown in Figure 4(c) and (d). Note that the observed rainfall anomalies clearly show the opposite polarity of anomaly pattern over Indian subcontinent and the EEIO for the six weak monsoon cases. On the other hand, the CFS OMF shows a rather poor simulation of the rainfall anomalies for the six weak monsoon cases. It is intriguing to note that the OMF fails to capture even the broad structure of this anomaly pattern associated with these major weak monsoon episodes. For the composite based on all the 16 weak monsoon cases,

the similarities in the rainfall and wind anomalies between the CMAP/NCEP datasets and CFS OMF seem to be poorer (Figure 4(e) and (f)).

SST anomalies for July 2002 based on the CFS OMF and GODAS are shown in Figure 5(a) and (b). Some aspects of the observed warm SST anomaly in the central-eastern tropical IO are seen in the OMF: However, the model completely fails to capture the warm SST anomalies in the Bay of Bengal and central-eastern Arabian Sea resulting from reduced upwelling and decreased evaporation due to the weakened southwesterly monsoon winds. In fact, the observed SST
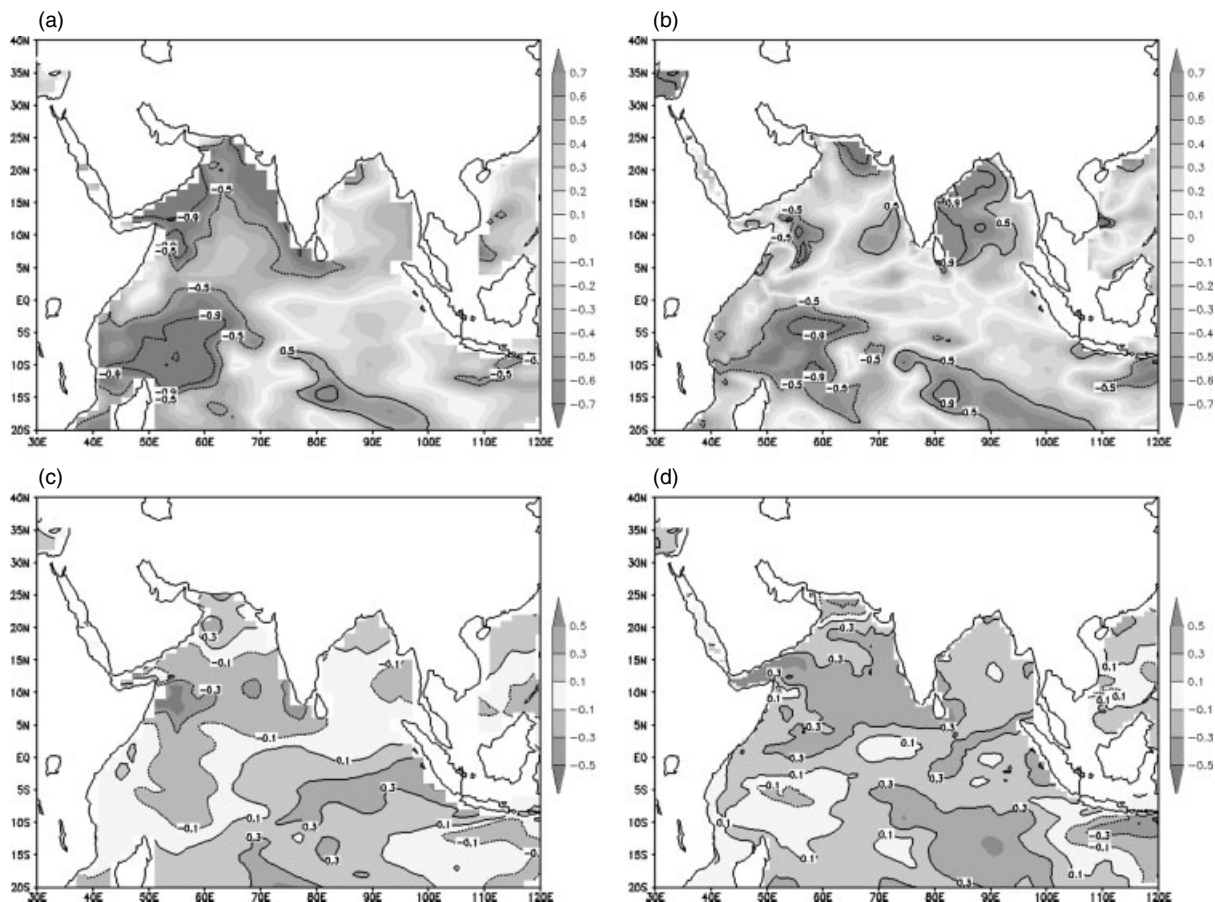
Figure 5. Sea surface temperature (SST) anomaly (°C) for; (a) CFS OMF during July 2002; (b) same as (a) but from GODAS; (c) mean of six week monsoon months (from table 5.1) CFS OMF; (d) same as (c) but from GODAS.

anomaly composite, based on the six weak monsoon cases, shows warm anomalies covering most parts of the Arabian Sea and Bengal (Figure 5(d)). The SST anomaly composite from the CFS OMF shows cold anomalies in the Arabian Sea and eastern Bay of Bengal (Figure 5(c)), indicating the inability of the CFS forecasts to capture the anomalous SST response associated with weakening of the monsoonal flow. Anomalies of 20 °C isotherm depth (D20) and mixed layer depth (MLD) during July 2002 are shown in Figure 6(a) and (b) for the OMF and GODAS respectively. The corresponding composites based on the six weak monsoon cases are shown in Figure 6(c) and (d). The anomalous deepening (shoaling) of D20 and MLD in the EEIO are qualitatively seen in the CFS OMF.

The above discussions point to some of the deficiencies in the CFS OMF in adequately capturing the weak monsoon anomalies, the Indian Ocean – monsoon feedbacks and the out-of-phase pattern of precipitation response over the Indian subcontinent and the EEIO. Current understanding suggests that the above model biases arise partly due to systematic errors in simulating the ocean-atmosphere interactive processes over the Indian Ocean, Arabian Sea and the Bay of Bengal. Here it is important to recognize that the nature of ocean-atmosphere coupling is not uniform throughout the IO basin. Ocean dynamics is crucial, particularly in the equatorial IO, and this feature is salient for producing a Bjerknes-type wind-thermocline feedback which governs the evolution of SST and precipitation anomalies in the equatorial IO region (e.g. Saji *et al.*, 1999; Webster *et al.*, 1999; Yamagata *et al.*, 2004; Annamalai *et al.*, 2005). Dynamical coupling between SST and

rainfall is not as strong over the central-eastern Arabian Sea as compared to the equatorial IO. In fact, observations during July 2002 support this argument (see Figures 4(b) and 5(b)). It can be noticed that the rainfall decrease over the Arabian Sea and Bay of Bengal during weak monsoons such as in July 2002 is accompanied by warm SST anomalies locally, thereby suggesting that the Arabian Sea SST anomalies mostly indicate a response to the monsoonal wind forcing. In fact, variations in the summer monsoon winds, surface net-heat and salt fluxes are known to exert considerable influence on the SST response in the Arabian Sea and Bay of Bengal (e.g. Annamalai *et al.*, 2005; Ramesh and Krishnan, 2005). Therefore, deficiencies in realistic representation of winds and moist convective processes over the Arabian Sea and Bay of Bengal, as well as improper treatment of ocean-atmosphere coupling, can lead to large errors in simulating rainfall and SST variations in this region (e.g. Levine and Turner, 2011).

3.3. Potential for improving monsoon simulations in CFS model

With regard to the scope for improving the monsoon simulations, one of the potential areas would be to improve the equatorial IO dynamical processes in the CFS model. Although the CFS model shows anomalous precipitation enhancement over the EEIO during weak Indian monsoons, the equatorial IO anomalies in the model are not strong enough to weaken the summer monsoon reverse Hadley circulation and suppress the monsoon rainfall over the Indian landmass. The zonal gradient of the mean D20 is an important feature that determines the
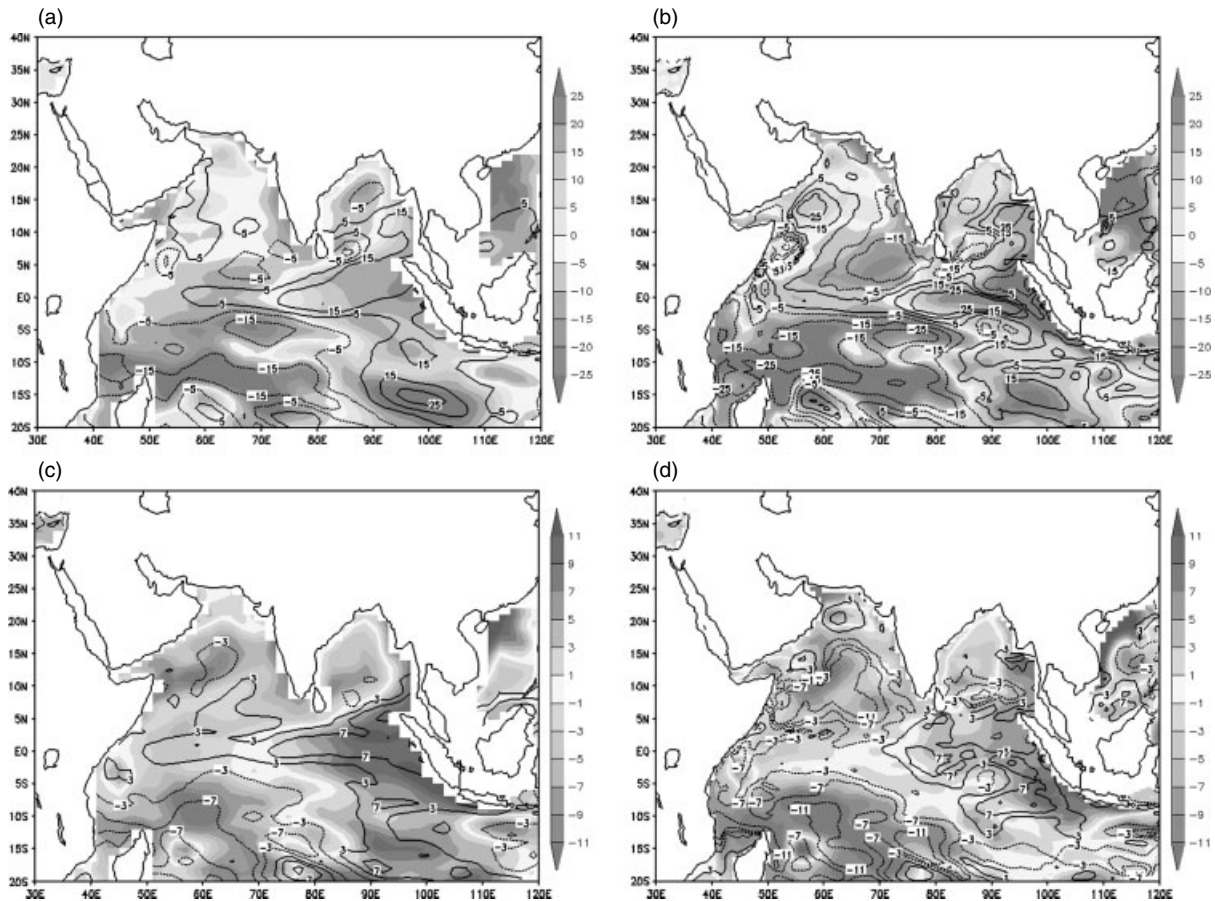
Figure 6. Depth at 20 °C isotherm (D20) anomaly (m) shaded and Mixed Layer Depth anomaly (m) contour for; (a) CFS OMF during July 2002; (b) same as (a) but from GODAS; (c) mean of six weak monsoon months CFS OMF; (d) same as (c) but from GODAS.

thermocline variations in the equatorial IO and the slow evolution of SST anomalies. To understand why the near-equatorial IO anomalies are not as strong in the CFS model, an examination of the structure of the ocean thermocline was carried out. Figure 7 shows the zonal variation of D20 averaged between 5 °N and 10 °S in the near-equatorial IO from the CFS model and GODAS dataset. It can be noticed that the D20 in CFS model is more-or-less flat, with a mean depth of about 108 m. On the other hand, the D20 in the GODAS dataset shows a gentle east–west slope which is deeper in the eastern IO as compared to the western IO.

Correcting the flat D20 in the CFS model can be a significant remedy towards improving the ocean–atmosphere coupled interactions in the equatorial IO, which in turn could lead to more realistic simulations of the monsoon rainfall variations. To check this hypothesis, outputs from a 100 year free run of the CFS coupled model are examined. While statistical models generally have limitations in predicting extremes (i.e. droughts/floods) in the monsoon rainfall (Gadgil *et al.*, 2005), it may be worthwhile to understand if the CFS model has the ability to simulate monsoon precipitation extremes and associated ocean–atmosphere coupled interactions. The free run is for an arbitrary 100 year period and this run was conducted as part of the seasonal monsoon prediction efforts at the Indian Institute of Tropical Meteorology. Figure 8 shows the time-series of interannual variability of the June–September summer monsoon rainfall over the Indian region (70–90 °E; 10–30 °N) from the free run. The mean and standard-deviation values of rain-rate in the CFS model are found to be 5.8
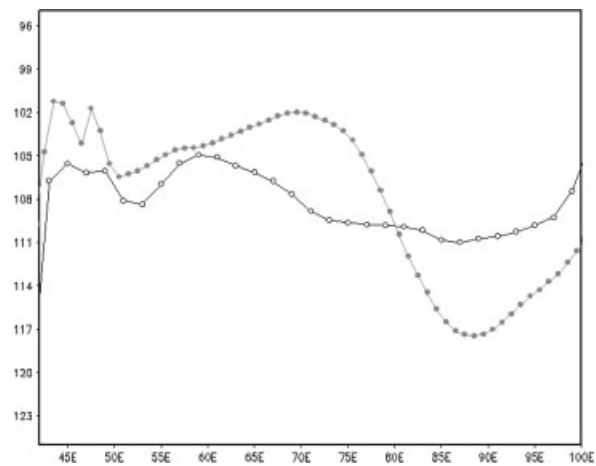

Figure 7. June, July, August, September mean climatological D20 depth (m) averaged from 10 °S to 5 °N *versus* longitude; (a) CFS OMF (open circle); (b) GODAS (filled circle).

and 0.82 mm day^{-1}, respectively. The corresponding values for the observed IMD gridded $1° \times 1°$ rainfall data over India (Rajeevan *et al.*, 2006) are 7.5 and 0.85 mm day^{-1}, respectively. It may be noted that the mean rainfall in the CFS model is underestimated compared to the IMD mean rainfall. This is partly because the mean monsoon rainfall over northeast India and the Bay of Bengal is underestimated in the CFS model. Also, it must be noted that IMD rainfall is based on
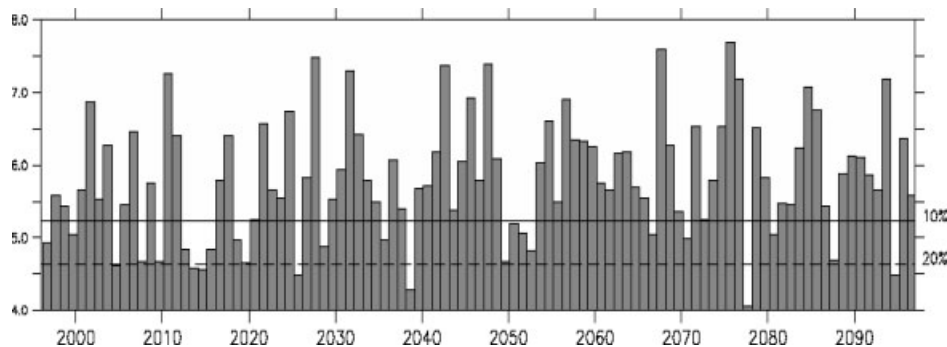
Figure 8. Time-series of interannual variability of the June–September summer monsoon rainfall (mm day^{-1}) over the Indian region (70–90 °E; 10–30 °N) from the free run of CFS from 1996 to 2096.
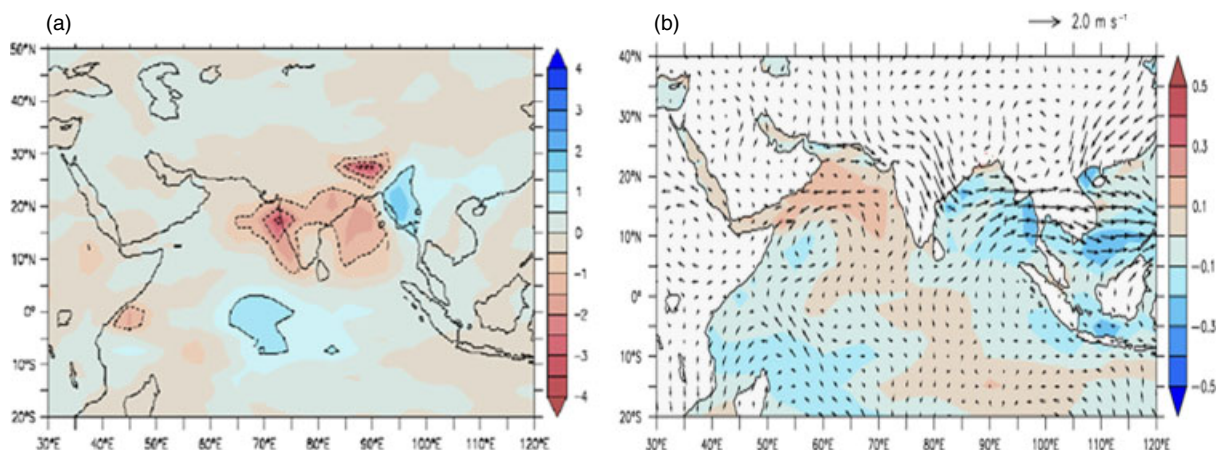

Figure 9. (a) The composite of rainfall anomalies (mm day^{-1}) based on all monsoon drought cases when the seasonal (June, July, August, September) monsoon rainfall anomaly over the Indian region (70–90 °E; 10–30 °N) was less than −10% of the climatological normal; (b) shows the corresponding anomaly composites for SST (°C) and 850 hPa winds (m s^{-1}). This figure is available in colour online at wileyonlinelibrary.com/journal/met

data over land points only, while the CFS rainfall includes both land and ocean points. However, the important issue is that the level of interannual variability of monsoon rainfall averaged over the Indian region is comparable in both the CFS model and the IMD dataset as seen from the standard deviation values.

In order to understand whether Indian monsoon droughts simulated in the 100 year free run of the CFS show features corresponding to the anomalous coupled interactions in the tropical IO, an analysis of rainfall, SST and low-level wind variations from the CFS free run was carried out for all the monsoon droughts simulated by the model. Figure 9(a) shows the composite of rainfall anomalies based on all the monsoon drought cases when the seasonal (JJAS) monsoon rainfall anomaly over the Indian region (70–90 °E; 10–30 °N) was less than −10% of the climatological normal. The corresponding anomaly composites for SST and 850 hPa winds are shown in Figure 9(b). The threshold of 10% departures from climatological normal is similar to the classification of excess and deficit monsoon rainfall seasons by the India Meteorological Department (IMD). It may be noted that the 10% threshold is roughly 1 standard deviation (∼85 mm) of the climatological mean seasonal (JJAS) AIR (see Parthasarathy *et al*., 1994). It can be seen that the monsoon rainfall deficiency over the Indian subcontinent is associated with a weakening of the southwest monsoon flow over the Arabian Sea and the formation of an anomalous ridge over South Asia. The warm SST anomalies in the Arabian Sea are consistent

with a weakened southwesterly monsoon flow. It is, however, important to note in Figure 9(a) and (b) that the rainfall and SST anomalies in the equatorial IO do not reveal appreciable changes. This might suggest that Indian monsoon droughts in the CFS model are not strongly linked with coupled interactions in the equatorial IO.

Intrigued by the above results, an examination was carried out to understand cases of very intense monsoon droughts simulated by the CFS model. In selecting intense monsoon droughts, only those cases were considered when deficiencies in the seasonal monsoon rainfall were below −20% of the climatological normal. Anomaly composites of rainfall, wind and SST based on the intense monsoon droughts are shown in Figure 10. It is quite interesting to note that the monsoon and IO coupled interactions stand out very prominently when the intense monsoon droughts are considered. The pattern of decreased rainfall over India and increased rainfall over the EEIO is rather striking in Figure 10(a). In addition to the weakening of the monsoonal flow, as evidenced from the anticyclonic anomaly over the Indian region, anomalous westerlies can be noticed over the equatorial IO. The SST anomaly composite (Figure 10(b)) based on the intense monsoon droughts shows anomalous warming (>0.5 °C) in the EEIO and cold anomalies in the western IO. The pattern of SST, wind and precipitation response in Figure 10 is indicative of a Bjerknes-type feedback in which a positive zonal SST gradient favours equatorial
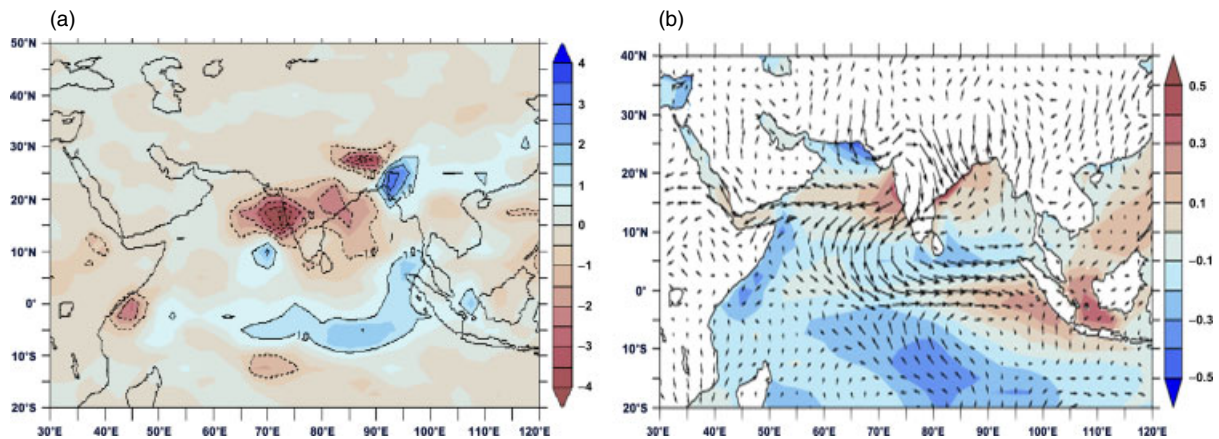
Figure 10. (a) The composite of rainfall anomalies (mm day^{-1}) based on all monsoon drought cases when the seasonal (June, July, August, September) monsoon rainfall anomaly over the Indian region (70–90 °E; 10–30 °N) was less than −20% of the climatological normal; (b) shows the corresponding anomaly composites for SST (°C) and 850 hPa winds (m s^{-1}). This figure is available in colour online at wileyonlinelibrary.com/journal/met

westerly anomalies, which in turn pushes warm waters to the east and sustains the warm SST anomalies in the region through downwelling and thermocline deepening.

The main message conveyed from the above discussions is that the CFS model seems to possess features inherent to coupled interactions between the monsoon flow and Indian Ocean dynamics. However, because of the flat near-equatorial thermocline in the CFS model, a great deal of effort would be required to trigger and maintain this coupled feedback process. Therefore, very often the equatorial IO anomalies in the CFS model are not strong enough to produce drought conditions over India through weakening of the monsoon Hadley cell. The role of equatorial IO coupled dynamics emerges out prominently only in the case of very intense monsoon droughts. Therefore, it is hoped that efforts to improve the structure of the mean thermocline in the CFS model (e.g. through better representation of vertical mixing), together with improvements in data assimilation for providing more realistic ocean initial conditions, would greatly benefit extended range predictions of the IO coupled dynamics and the evolution of monsoonal rains on the intra-seasonal time-scale.

4. Summary

The work presented in this paper is an assessment and validation of ensemble 1 month forecast (OMF) by the NCEP CFS coupled model. In particular, the skill of the CFS OMF in capturing weak monsoons was investigated using the CFS hindcasts (retrospective-forecasts) available for a 28 year period (1981–2008). The weak monsoons in this study correspond to periods when the monthly all India rainfall anomaly during the summer monsoon months was >−20% of the climatological normal. There were 16 such weak monsoon cases during (1981–2008). Examination of the CFS OMF for these 16 weak monsoon cases showed that the rainfall and circulation anomalies were poorly captured by the model. In general, the correlation between the observed rainfall and OMF over the Indian monsoon region is found to be poor. By performing detailed analyses, it is noted that deficiencies in realistically capturing the ocean-atmosphere coupling in the near-equatorial Indian Ocean (IO) gives rise to biases in simulating the SST and rainfall anomalies in the equatorial region, which in turn affects

the monsoon precipitation forecasts over the subcontinent. In particular, it is noted that the equatorial IO anomalies simulated by the CFS model are unable to induce large-scale rainfall deficiencies over the Indian subcontinent. Furthermore, the systematic biases in simulating the wind, rainfall and SST variations in the Arabian Sea and Bay of Bengal result in errors in the OMF of monsoon rainfall over India.

NCEP has released the recent version (v2) of the CFS model in 2010 and the ensemble hindcasts (reforecasts) from CFS-v2 are available for the period 1981–2010. A preliminary analysis was carried out to see the skill of the OMF of weak monsoons from the CFS-v2 simulations. Although some improvements are noted in the simulation of SST and rainfall anomalies over the equatorial Indian Ocean in the CFS-v2 model during weak monsoons, the link between the equatorial anomalies and the Indian monsoon rainfall anomalies is not adequately captured even in the CFS-v2 version (figures not shown). Pattanaik and Kumar (2010) pointed out that the skill of the CFS-v1 model in simulating the Indian Ocean Dipole is rather poor largely due to cold SST bias in the eastern equatorial Indian Ocean. One of the potential areas for enhancing the quality of monsoon forecasts in the CFS model is to improve the thermocline structure in the near-equatorial IO. The flat thermocline in the CFS model does not sustain the Bjerknes-type wind-thermocline feedback effectively, leading to weaker equatorial anomalies and weaker teleconnections with the Indian monsoon rainfall. In fact, this point has been confirmed by a careful examination of a 100 year free run of the CFS coupled model. It is seen that moderate monsoon droughts produced by the CFS model have weak linkage with the equatorial IO dynamics, although it is interesting to note that very intense monsoon droughts simulated by the CFS model had remarkable teleconnections with the equatorial anomalies. Based on these points, it is suggested that improving the structure of the mean thermocline in the CFS model, together with developments in ocean data-assimilation, offers good prospects for advancing the skill of extended range monsoon predictions using the CFS model.

Additionally, improvements in parameterization of moist convection can greatly help in minimizing the monsoon precipitation biases over South Asia and the adjoining oceanic areas. Zhou et al. (2012) have proposed modifications in the convection scheme of the CCSM3 model, involving convective momentum transport and direct plume approximation, which

lead to improved simulation of the Madden Julian Oscillation. Their results indicate that the modified convection scheme reduces the easterly wind bias in the Indian Ocean and western Pacific Ocean. It would be worthwhile investigating whether similar modifications in convection scheme of the CFS model can help reduce the biases in the eastern Indian Ocean (i.e. easterly winds, cold SST and shallow thermocline), thereby leading to improved forecasts of the Indian monsoon

Acknowledgements

References

Annamalai H, Potemra J, Murtugudde R, McCreary JP. 2005. Effect of preconditioning on the extreme climate events in the tropical Indian Ocean. *J. Clim.* **18**: 3450–3469.

Behera SK, Luo JJ, Masson S, Rao SA, Sakuma H, Yamagata T. 2006. A CGCM study on the interaction between IOD and ENSO. *J. Clim.* **19**: 1688–1705.

Bhat GS. 2006. The Indian drought of 2002 – a sub-seasonal phenomenon? *Q. J. R. Meteorol. Soc.* **132**: 2583–2602.

Cadet DL, Daniel P. 1988. Long-range forecast of the break and active summer monsoons. *Tellus-A* **40**: 131–150.

Chattopadhyay R, Sahai AK, Goswami BN. 2008. Objective identification of nonlinear convectively coupled phases of monsoon intraseasonal oscillation. Implications for prediction. *J. Atmos. Sci.* **65**: 1549–1569.

Chen TC, Yen MC, Wu KD, Thomas NG. 1992. Long-range prediction of the low-frequency mode in the low-level Indian monsoon circulation with a simple statistical method. *Tellus A* **44A**: 324–330.

Drbholav H-KL, Krishnamurthy V. 2010. Spatial structure, forecast errors and predictability of the South Asian monsoon in CFS monthly retrospective forecasts. *J. Clim.* **23**: 4750–4769.

Ferranti L, Palmer TN, Molteni F, Klinker E. 1990. Tropical-extratropical interaction associated with the 30–60 day oscillation and its impact on medium and extended range prediction. *J. Atmos. Sci.* **47**: 2177–2199.

Fu X, Wang B, Waliser DE, Tao L. 2007. Impact of atmosphere-ocean coupling on the predictability of monsoon intraseasonal oscillations. *J. Atmos. Sci.* **64**(1): 157–174.

Gadgil S, Rajeevan M, Nanjundiah R. 2005. Monsoon prediction – Why yet another failure? *Curr. Sci.* **88**(9): 1389–1400.

Goswami BN. 2005. South Asian monsoon. In *Intraseasonal Variability of the Atmosphere-Ocean Climate System*, Lau WKM, Waliser DE (eds). Chapter 2. Praxis, Springer: Berlin, Heidelberg; 19–61.

Goswami BN, Ajaya Mohan RS. 2001. Intraseasonal oscillations and interannual variability of the Indian summer monsoon. *J. Clim.* **14**: 1180–1198.

Joseph S, Sahai AK, Goswami BN. 2009. Eastward propagating MJO during boreal summer and Indian monsoon droughts. *Clim. Dyn.* **32**: 1139–1153, DOI: 10.1007/s00382-008-0412-8.

Joseph S, Sahai AK, Goswami BN. 2010. Boreal summer intraseasonal oscillations and seasonal Indian monsoon prediction in DEMETER coupled models. *Clim. Dyn.* **35**: 651–667, DOI 10.1007/s00382-009-0635-3.

Kanamitsu M, Ebisuzaki W, Woollen J, Yang SK, Hnilo JJ, Fiorino M, Potter GL. 2002. NCEP–DOE AMIP-II reanalysis (R-2). *Bull. Am. Meteorol. Soc.* **83**: 1631–1643.

Kang IS, Shukla J. 2005. Dynamical seasonal prediction and predictability of monsoon. In *The Asian Monsoon*. Wang B (ed.). Praxis Pub. Ltd: Chichester, UK.

Kripalani RH, Singh SV, Arkin PA. 1991. Large-scale features of rainfall and outgoing long-wave radiation over Indian and adjoining regions. *Atmos. Phys.* **64**: 159–168.

Krishna Kumar K, Hoerling M, Rajagopalan B. 2005. Advancing dynamical prediction of Indian monsoon rainfall. *Geophys. Res. Lett.* **32**: 1–4.

Krishnamurti TN, Oosterhof DK, Mehta VK. 1988. Air–Sea interaction on the time scale of 30–50 days. *J. Atmos. Sci.* **45**(8): 1304–1322.

Krishnamurti TN, Subrahmanyam D. 1982. The 30–50 day mode at 850 mb during MONEX. *J. Atmos. Sci.* **39**: 2088–2095.

Krishnamurti TN, Subramaniam M, Daughenbaugh G, Oosterhof D, Xue JH. 1992. One-month forecasts of wet and dry spells of the monsoon. *Mon. Weather Rev.* **120**: 1191–1223.

Krishnamurti TN, Subramaniam M, Oosterhof DK, Daughenbaugh G. 1990. Predictability of low-frequency modes. *Meteorol. Atmos. Phys.* **44**: 63–83.

Krishnamurti TN, Thomas A, Simon A, Kumar V. 2010. Desert air incursions, an overlooked aspect, for the dry spells of the Indian summer monsoon. *J. Atmos. Sci.* **67**: 3423–3441.

Krishnan R, Kumar V, Sugi M, Yoshimura J. 2009. Internal feedbacks from monsoon-midlatitude interactions during droughts in the Indian summer monsoon. *J. Atmos. Sci.* **66**(3): 553–578.

Krishnan R, Mujumdar M, Vaidya V, Ramesh KV, Satyan V. 2003. The abnormal Indian summer monsoon of 2000. *J. Clim.* **16**: 1177–1194.

Krishnan R, Ramesh KV, Samala BK, Meyers G, Slingo JM, Fennessy MJ. 2006. Indian Ocean-monsoon coupled interactions and impending monsoon droughts. *Geophys. Res. Lett.* **33**: L08711, DOI: 10.1029/2006GL025811.

Krishnan R, Sundaram S. 2007. On the dynamical extended range predictability of active/break spells of the Indian summer monsoon. Sensitivity to atmospheric initial conditions. *Int. J. Ecol. Dev.* **3**: 1–25.

Krishnan R, Sundaram S, Swapna P, Kumar V, Ayantika DC, Mujumdar M. 2011. The crucial role of ocean-atmosphere coupling on the Indian monsoon anomalous response during dipole events. *Clim. Dyn.* **37**: 1–17.

Krishnan R, Swapna P. 2009. Significant influence of the boreal summer monsoon flow on the Indian Ocean response during dipole events. *J. Clim.* **22**: 5611–5634.

Krishnan R, Zhang C, Sugi M. 2000. Dynamics of breaks in the Indian summer monsoon. *J. Atmos. Sci.* **57**(9): 1354–1372.

Kulkarni AA, Kripalani RH, Sabade S, Rajeevan M. 2011. Role of intra-seasonal oscillations in modulating the Indian summer monsoon rainfall. *Clim. Dyn.* **36**: 1005–1021.

Levine RC, Turner AG. 2011. Dependence of Indian monsoon rainfall on moisture fluxes across the Arabian Sea and the impact of coupled model sea surface temperature biases. *Clim. Dyn.* ISSN 0930–7575.

Luo JJ, Masson S, Behera SK, Yamagata T. 2007. Experimental forecasts of the Indian Ocean dipole using a coupled OAGCM. *J. Clim.* **20**: 2178–2190.

Luo JJ, Masson S, Behera SK, Yamagata T. 2008a. Extended ENSO predictions using a fully coupled ocean–atmosphere model. *J. Clim.* **21**: 84–93.

Luo JJ, Behera SK, Masumoto Y, Sakuma H, Yamagata T. 2008b. Successful prediction of the consecutive IOD in 2006 and 2007. *Geophys. Res. Lett.* **35**: L14S02.

Moorthy KK, Saha A, Prasad BSN, Niranjan K, Jhurry D, Pillai PS. 2001. Aerosol optical depths over peninsular India and adjoining oceans during the INDOEX campaigns. Spatial, temporal, and spectral characteristics. *J. Geophys. Res.* **106**(D22): 28,539–28,554.

Neena JM, Suhaas E, Goswami BN. 2011. Leading role of internal dynamics in the 2009 Indian summer monsoon drought. *J. Geophys. Res* **116**: D13103, DOI: 101029/2010JD015328.

Pacanowski RC, Griffies SM. 1998. *MOM 3.0 Manual*. NOAA/Geophysical Fluid Dynamics Laboratory: Princeton, NJ.

Palmer TN, Alessandri A, Andersen U, Cantelaube P, Davey M, Delecluse P, Deque M, Diez E, Doblas-Reyes FJ, Feddersen H, Graham R, Gualdi S, Gueremy JF, Hagedorn R, Hoshen M, Keenlyside N, Latif M, Lazar A, Maisonnave E, Marletto V, Morse AP, Orfila B, Rogel P, Terres JM, Thomson MC. 2004. Development of a European multi-model ensemble system for seasonal to inter-annual prediction (DEMETER). *Bull. Am. Meteorol. Soc.* **85**: 853–872.

Parthasarathy B, Munot AA, Kothawale DR. 1994. All-India monthly and seasonal rainfall series. 1871–1993. *Theor. Appl. Climatol.* **49**: 217.

Pattanaik DR, Kumar A. 2010. Prediction of summer monsoon rainfall over India using the NCEP climate forecast system. *Clim. Dyn.* **34**: 557–572.

Rajeevan M, Bhate J, Kale JD, Lal B. 2006. High resolution daily gridded rainfall data for the Indian region: analysis of break and active monsoon spells. *Curr. Sci.* **91**(3): 296–306.

Ramaswamy C. 1962. Breaks in the Indian monsoon as a phenomenon of interaction between easterly and the subtropical westerly jet streams. *Tellus* **14**: 337–349.

Ramesh KV, Krishnan R. 2005. Coupling of mixed layer processes and thermocline variations in the Arabian Sea. *J. Geophys. Res.* **110**: c05005, DOI: 10.1029/2004JC002515.

Roxy M, Tanimoto Y. 2007. Role of SST over the Indian Ocean in influence the intraseasonal variability of the Indian summer monsoon. *J. Meteorol. Soc. Jpn.* **85**(3): 349–358.

Roxy M, Tanimoto Y. 2011. Influence of sea surface temperature on the intraseasonal variability of the South China Sea summer monsoon. *Clim. Dyn.* DOI: 10.1007/s00382-011-1118-x.

Saji NH, Goswami BN, Vinayachandran PN, Yamagata T. 1999. A dipole mode in the tropical Indian Ocean. *Nature* **401**(6751): 360–363.

Saha S, Nadiga S, Thiaw C, Wang J, Wang W, Zhang Q, van den Dool HM, Pan HL, Moorthi S, Behringer D, Stokes D, Pena M, Lord S, White G, Ebisuzaki W, Peng P, Xie P. 2006. The NCEP climate forecast system. *J. Clim.* **19**: 3483–3517.

Saith N, Slingo JM. 2006. The role of Madden-Julian Oscillation in the El Nino and Indian drought of 2002. *Int. J. Climatol.* **26**: 1361–1378.

Sengupta D, Ravichandran M. 2001. Oscillations of Bay of Bengal sea surface temperature during the 1998 summer monsoon. *Geophys. Res. Lett.* **28**(10): 2033–2036.

Sikka DR. 1999. Monsoon drought in India joint. COLA/CARE Technical Report No. 2, Centre for Ocean-Land Atmosphere studies, Calverton, MD.

Sikka DR, Gadgil S. 1980. On the maximum cloud zone and the ITCZ over Indian longitudes during the West coast monsoon. *Mon. Weather Rev.* **108**: 1840–1853.

Singh SV, Kripalani RH. 1985. The south to north progression of rainfall anomalies across India during the summer monsoon season. *Pure Appl. Geophys.* **123**: 624–637.

Vecchi G, Harrison DE. 2002. Monsoon breaks and subseasonal sea surface temperature variability in the Bay of Bengal. *J. Clim.* **15**: 1485–1493.

Vitart F. 2004. Monthly forecasting at ECMWF. *Mon. Weather Rev.* **132**: 2761–2779.

Vitart F, Molteni F. 2009. Simulation of the MJO and its teleconnections in an ensemble of 46 day EPS hindcasts. *ECMWF Tech. Memo.* **597**: 60.

Waliser DE, Stern W, Schubert S, Lau KM. 2003. Dynamic predictability of intraseasonal variability associated with the Asian summer monsoon. *Q. J. R. Meteorol. Soc.* **129**: 2897–2925.

Wang B, Ding QH, Fu XH, Kang IS, Jin K, Shukla J, Doblas-Reyes F. 2005. Fundamental challenge in simulation and prediction of summer monsoon rainfall. *Geophys. Res. Lett.* **32**: L15711.

Wang B, Xie X. 1997. A model for the boreal summer intraseasonal oscillation. *J. Atmos. Sci.* **54**(1): 71–86.

Webster PJ, Hoyos C. 2004. Forecasting monsoon rainfall and river discharge variability on 20–25 day time scales. *Bull. Am. Meteorol. Soc.* **85**: 1745–1765.

Webster PJ, Moore AM, Loschnigg JP, Leben RR. 1999. Coupled ocean-atmosphere dynamics in the Indian Ocean during 1997–1998. *Nature* **401**: 356–360.

Xavier PK, Goswami BN. 2007. An analog method for real-time forecasting of summer monsoon subseasonal variability. *Mon. Weather Rev.* **135**: 4149–4160.

Xie P, Arkin PA. 1996. Analyses of global monthly precipitation using gauge observations, satellite estimates, and numerical model predictions. *J. Clim.* **9**: 840–858.

Yamagata T, Behera SK, Luo JJ, Masson S, Jury M, Rao SA. 2004. Coupled ocean atmosphere variability in the tropical Indian Ocean, in Earth Climate. In *The Ocean-Atmosphere Interaction, Geophysical Monograph Series, Vol. 147*, Wang C, Xie S-P, Carton JA (eds). AGU: Washington, DC; 189–212.

Yasunari T. 1979. Cloudiness fluctuations associated with the northern hemisphere summer monsoon. *J. Meteorol. Soc. Jpn* **57**(3): 227–242.

Zhou L, Neale R, Jochum M, Murtugudde R. 2012. Improved Madden-Julian Oscillations with improved physics: the impact of modified convection parameterizations. *J. Clim.* **25**: 1116–1136.